Bioconjugate Chemistry

Article

pubs.acs.org/bc

Troponin T Immunosensor Based on Liquid Crystal and Silsesquioxane-Supported Gold Nanoparticles

Eduardo Zapp,*[,†] Paulo Sérgio da Silva,[‡] Eduard Westphal,[§] Hugo Gallardo,[§] Almir Spinelli,[‡] and Iolanda Cruz Vieira[†]

[†]Laboratory of Biosensors, [‡]Study Group of Electrochemical and Electroanalytical Processes, and [§]Laboratory of Synthesis of Liquid Crystals, Department of Chemistry, Federal University of Santa Catarina, 88040-900, Florianópolis, SC, Brazil

ABSTRACT: A nanostructured immunosensor based on the liquid crystal (*E*)-1-decyl-4-[(4-decyloxyphenyl)diazenyl]pyridinium bromide (Br-Py) and gold nanoparticles supported by the water-soluble hybrid material 3-*n*-propyl-4-picolinium silsesquioxane chloride (AuNP-Si4Pic$^+$Cl$^-$) was built for the detection of troponin T (cTnT), a cardiac marker for acute myocardial infarction (AMI). The functionalized nanostructured surface was used to bind anti-cTnT monoclonal antibodies through electrostatic interaction. The immunosensor (ab-cTnT/AuNP-Si4Pic$^+$Cl$^-$/Br-Py/GCE) surface was characterized by microscopy techniques. The electrochemical behavior of the immunosensor was studied by cyclic voltammetry and electrochemical impedance spectroscopy. A calibration curve was obtained by square-wave voltammetry. The immnunosensor provided a limit of detection of 0.076 ng mL^{-1} and a linear range between 0.1 and 0.9 ng mL^{-1} (appropriate for AMI diagnosis).

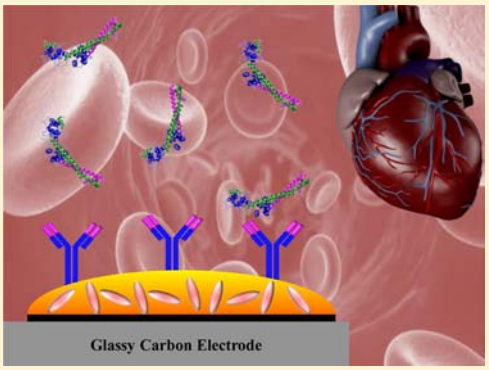

INTRODUCTION

Liquid crystals (LCs) are a class of materials in a physical state which lies between the crystalline solid and liquid phases.[1] They have been widely used in developmental research in several scientific and technological fields, with increasing application in electro-optical devices,[2−5] their use in displays being the most recognized form of application. In recent years, LC materials have also attracted great interest in relation to many other technological applications, but little attention has been given to the construction of biosensors. It has been previously reported that ionic LC molecules can be efficiently applied in redox probes for the determination of some phenolic compounds[6] and also in label-free immunosensors.[7] The property employed in the latter case is the ability of immune complexes to block the redox probe electron transfer process on the electrode surface, and thus the LC-based sensors can provide effective, simple, and promising tools for detection applications that do not require labeled analytes.[2,7,8]

Furthermore, Au nanoparticles (AuNPs) have received considerable attention in several fields due to their remarkable and unique properties which are not available in their bulk equivalent, such as high surface area/volume ratio and quantum confinement effects.[9] In addition, AuNPs have shown good biocompatibility, making them highly advantageous in the immobilization of biomolecules, such as enzymes and proteins, in electrochemical systems.[9−11] Several papers have reported the use of AuNPs for biosensor construction, increasing the direct electron transfer between the proteins and the electrodes.[10,12] However, these nanoparticles have a strong tendency to agglomerate and are not stable in aqueous dispersions. Thus, the synthesis of AuNPs requires the use of stabilizing agents to avoid their aggregation.[9]

Some authors have reported that soluble charged silsesquioxanes may offer an attractive alternative to support and stabilize metallic nanoparticles.[13−16] These materials show excellent performance in the adsorption of anionic metal complexes, such as $AuCl_4^-$ ions, and this allows small AuNPs, well-dispersed in aqueous medium, to be obtained. Other very important characteristics of silsesquioxanes are their capacity to form stable thin films on several surfaces, good electrical conductivity, and high stability.[13,15]

The diagnosis of cardiac disorders is of great importance given that the incidence of acute myocardial infarction (AMI) is associated with a very high mortality rate. For this reason, many studies have been conducted to shorten the time required for AMI diagnosis. Given the complex pathophysiology of heart disease, interest in plasma biochemical markers to predict susceptibility and aid in patient management has intensified.[17] After an AMI has occurred, cardiac biomarkers such as myoglobin, troponin I (cTnI), troponin T (cTnT), and creatine kinase (CK-MB) are released into the bloodstream and therefore their detection in serum can aid an accurate AMI diagnosis.[17,18]

Several methods of cTnT detection for AMI diagnosis have been described in the literature, including electrochemiluminescence immunoassay (ECLIA), enzyme-linked immunosorbent assay (ELISA), radioimmunoassay (RIA), and immuno-

Received: June 6, 2014
Published: August 11, 2014

dx.doi.org/10.1021/bc500341a | *Bioconjugate Chem.* 2014, 25, 1638−1643

chromatographic tests.[18−20] Recently, electrochemical immunosensor technology has become an important tool in disease diagnosis; however, most of the devices are still in the research phase.[17,21] The main advantage of electrochemical immunosensors is that their selectivity/specificity is associated with easy transducer operation.[17,18,21]

This paper reports the application of the ionic liquid crystal (*E*)-1-decyl-4-[(4-decyloxyphenyl)diazenyl]pyridinium bromide (Br-Py) and gold nanoparticles (AuNP) stabilized in a water-soluble 3-*n*-propyl-4-picolinium silsesquioxane chloride (Si4Pic$^+$Cl$^-$) matrix for the development of a new electrochemical immunosensor for the cardiac protein troponin. The immunosensor was optimized and applied in the detection and quantification of cTnT.

RESULTS AND DISCUSSION

Principle of Functioning. Figure 1 shows a schematic representation of the structural modification of a GCE using Br-Py molecules, AuNP-Si4Pic$^+$Cl$^-$ with immobilized ab-cTnT, and glycine blocking of nonspecific sites.

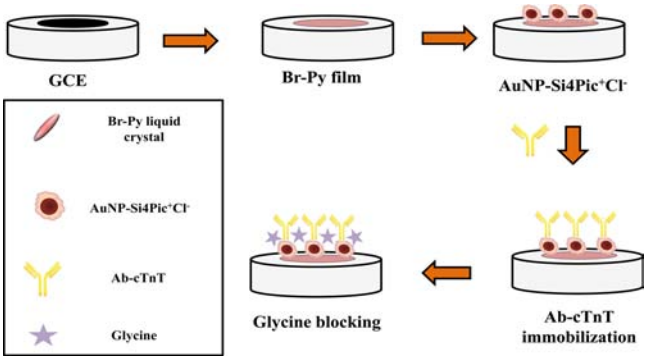

Figure 1. Steps involved in the immunosensor preparation.

The sensing principle for the detection of cTnT using the immunosensor is based on the voltammetric inhibition peak of Br-Py, which may be related to the azo group conjugated to the heterocycles of the Br-Py structure,[7] when cTnT molecules bind to the electrode surface. The immunocomplex formation was monitored by SWV. This immunocomplex formation is responsible for the partial blockage of the electroactive surface (Figure 2), compared with that obtained for the blank assay (base peak). First, an SWV measurement was taken using the immunosensor in PBS solution to obtain the base voltammetric peak (absence of cTnT). Subsequently, the immunosensor was incubated with 3 μL of cTnT sample for 10 min. After each step of the immunoassay the electrode surface was thoroughly washed with PBS (0.01 mol L^{-1}, pH 7.5) and a second voltammetric peak was obtained. The degree of inhibition of the peak was correlated with the cTnT concentration.

Immunosensor Surface. FEG-SEM analysis was carried out in order to examine the morphology of the sensor surface. Figure 3 shows the FEG-SEM micrographs obtained for different steps of the sensor construction. Figure 3A shows the surface of a bare GCE and Figure 3B the fiber-like texture of the GCE surface covered with Br-Py film. In Figure 3C ab-cTnT molecules immobilized on a surface composed of Br-Py film covered with AuNP-Si4Pic$^+$Cl$^-$ can be observed. Finally, in Figure 3D it is clear that a change in the texture occurs, indicating the presence of Gly molecules, which block the free sites of the electrode surface and inhibit the nonspecific adsorption of molecules.

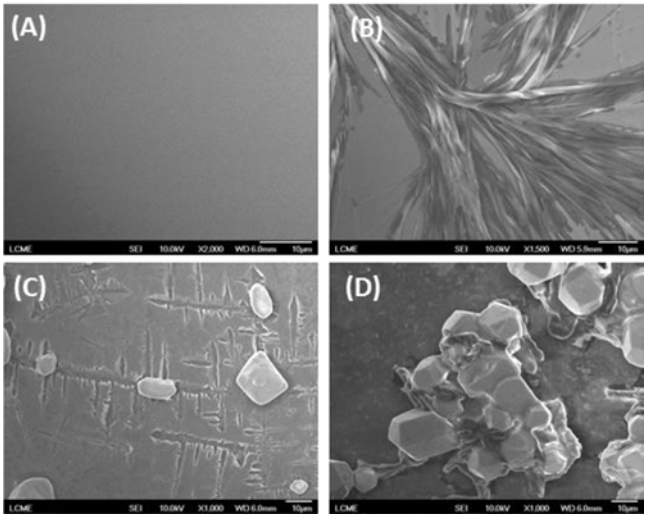

Figure 3. FEG-SEM micrographs of the (A) GCE, (B) Br-Py/GCE, (C) ab-cTnT/AuNP-Si4Pic$^+$Cl$^-$/Br-Py/GCE, and (D) gly/ab-cTnT/AuNP-Si4Pic$^+$Cl$^-$/ Br-Py/GCE samples observed at 10 kV.

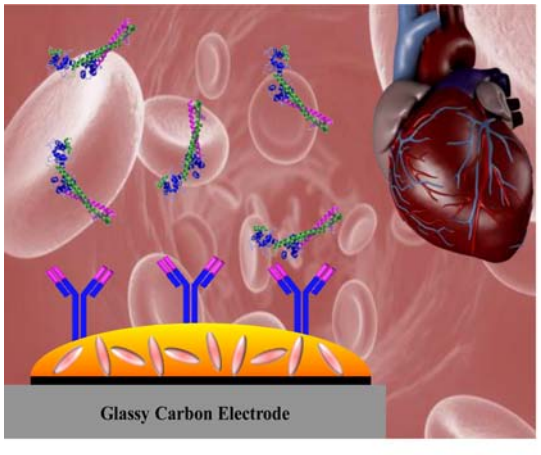

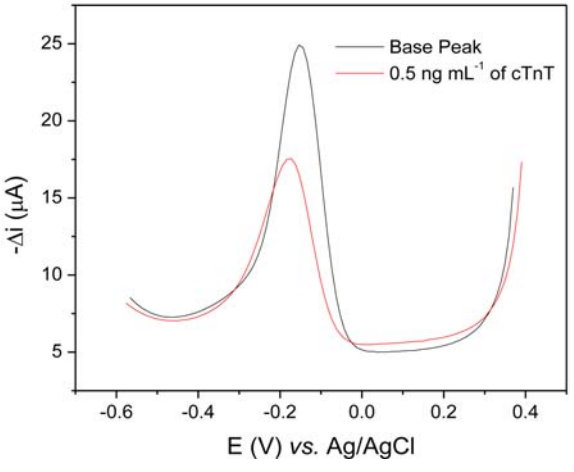

Figure 2. Schematic representation showing a proposal for the operating principle of the immunosensor.

dx.doi.org/10.1021/bc500341a | *Bioconjugate Chem.* 2014, 25, 1638−1643

It is assumed that the formation of conjugates occurs due to electrostatic interaction between the positively charged metal nanoparticles in the presence of the 4-picolinium group and the negative charge of the ab-cTnT. The decrease in the zeta potential values from +55 mV (AuNP-Si4Pic$^+$Cl$^-$) to +28 mV (AuNP-Si4Pic$^+$Cl$^-$/ab-cTnT) corroborates this assumption.

Optimization of the Sensor Construction. In order to optimize the construction process and the experimental conditions of the proposed immunosensor, some parameters were investigated using SWV. The Br-Py acts as a redox probe while the AuNPs improve the charge transfer process. The Br-Py also aids the immobilization of cTnT, resulting in improved sensor sensitivity. After the optimization of the immunosensor platform construction, the effects of varying the supporting electrolyte pH (3.0−9.0) in terms of the analytical properties of the immunosensor were investigated by EIS (for more details vide infra and Figure 4). Finally, the SWV parameters,

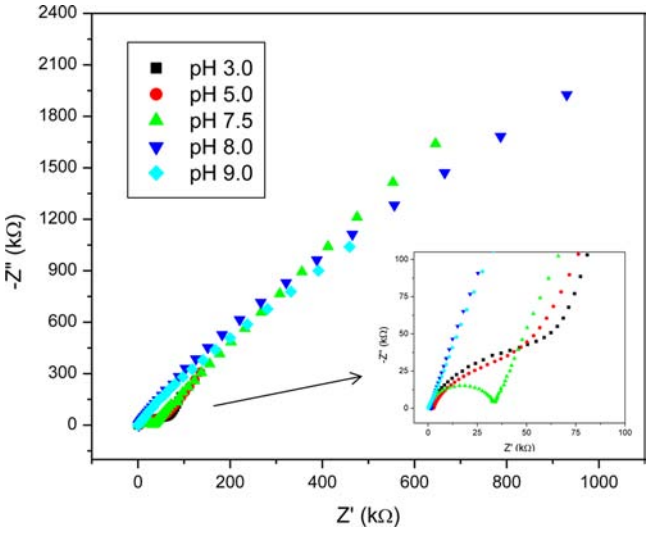

Figure 4. Influence of pH on immobilization of anti-troponin antibody by EIS.

frequency (10−100 Hz), amplitude (10−100 mV), and step potential (1−10 mV), were optimized to obtain the best immunosensor performance. The optimized parameters are summarized in Table 1 and these were used for cTnT detection.

Table 1. Summary of Optimization Parameters Evaluated and the Best Responses

parameter	range	best response
Br-Py quantity (mmol L^{-1})	0.1−1.0	1.0
AuNP-Si4Pic$^+$Cl quantity (μL)	1−4	3
Frequency (Hz)	10−100	100
Amplitude (mV)	10−100	80
Step potential (mV)	1−10	10
pH	3.0−9.0	7.5

The electrolyte solution pH can also affect the antibody immobilization by physical adsorption.[22] This dependence may be related to the differences in the charge and the degree of hydrophobicity of the variable regions of antibodies that may determine the orientation and conformational state of antibody molecules, which are dependent on the conditions of their adsorption.[23] Figure 4 shows the electrochemical impedance spectra for different pH values. As can be clearly observed, the pH has a major effect on the dynamic adsorption and also the amount adsorbed. The highest adsorption occurred at around pH 7.5 (the value used for analytical applications) based on the well-defined impedance semicycle, showing that this pH value is favorable to antibody immobilization on the modified AuNP-Si4Pic$^+$Cl electrode surface. At pH 3.0−5.0 good antibody adsorption was also observed, but this pH range is not appropriate for direct biological analysis. At more alkaline pH values the adsorption of the antibody was not observed.

Electrochemical Behavior. The electrochemical behavior of the stepwise immunosensor construction was investigated by cyclic voltammetry (Figure 5A). As expected, for the bare GCE (curve a), when the potential was varied in the range of +0.6 V to −0.6 V, no redox peak was observed. After the Br-Py immobilization (curve b), it is possible to observe the appearance of a pair of redox peaks, possibly due to the presence of the azo group conjugated to the benzene and pyridinium heterocycle of the Br-Py structure.[7] In the next step, when the AuNPs were immobilized on the Br-Py surface (curve c) a small decrease in the peak-to-peak separation was observed, evidencing that the thermodynamics of Br-Py charge transfer process was improved.[16] It can also be observed in Figure 5A that after immobilization of the ab-cTnT (curve d) and Gly (curve e) the redox peaks were suppressed. These results indicate a decrease in the faradaic process attributed to changes occurring at the sensor surface due to the insulation provided by the protein and amino acid molecules.[24] Therefore, the voltammetric responses clearly indicate an alteration in the dynamics of the charge transfer on the sensor surface. Electrochemical impedance spectroscopy (EIS) was also used to evaluate the charge transfer resistance (R_{ct}) for each step of the immunosensor construction.

Figure 5B shows the Nyquist plots (Z'' vs Z') obtained for (a) GCE, (b) Br-Py/GCE, (c) AuNP-Si4Pic$^+$Cl$^-$/Br-Py/GCE, (d) ab-cTnT/AuNP-Si4Pic$^+$Cl$^-$/Br-Py/GCE, and (e) gly/ab-cTnT/AuNP-Si4Pic$^+$Cl$^-$/Br-Py/GCE in a 0.1 mol L^{-1} KCl solution containing 5 mmol L^{-1} $Fe(CN)_6^{3-/4-}$. The semicircle in the Nyquist plots is characteristic of a Randles circuit which includes the ohmic resistance of the electrolyte solution (R_s), the Warburg impedance (Z_w), the double layer capacitance (C_{dl}), and the R_{ct}. The R_{ct} values obtained were as follows: bare GCE (1.2 kΩ), Br-Py/GCE (5.0 kΩ), AuNP-Si4Pic$^+$Cl$^-$/Br-Py/GCE (8.5 kΩ), ab-cTnT/AuNP-Si4Pic$^+$Cl$^-$/Br-Py/GCE (15.5 kΩ), and ab-Mb/AuNP-PEI/Br-Py/GCE (20.5 kΩ). The semicircles obtained at lower frequency represent a diffusion-limited electron transfer process and those at higher frequency represent a charge transfer-limited process.[25] As can be observed, each modification step promoted a significant increase in the R_{ct} of the electrodes, reflected by an increase in the semicircle size, verifying that the electrode surface was modified. The greatest increase in R_{ct} occurred in the presence of protein molecules (spectrum d), which is consistent with the voltammetry functioning principle where the signal suppression can be attributed to the insulating nature of ab-TnT (voltammogram d).

cTnT Calibration Curve, Reproducibility, and Stability. Figure 6 shows the calibration curve obtained with an increasing concentration of cTnT between 0.1 and 0.9 ng mL^{-1}, using SWV within the potential range of 0.6 to −0.6 V. The regression equation for the straight line obtained is I.P. = 2.4 (±1.4) + 55.2 (±2.4) [cTnT], with a correlation coefficient

dx.doi.org/10.1021/bc500341a | Bioconjugate Chem. 2014, 25, 1638−1643

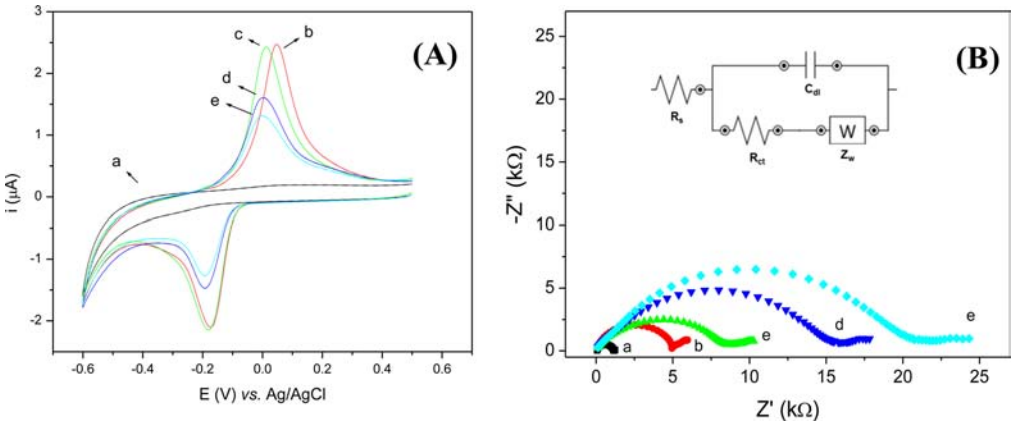

Figure 5. Electrochemical behavior: (A) Cyclic voltammograms at 100 mV s^{-1} and (B) Nyquist plots obtained by electrochemical impedance spectroscopy (EIS) for (a) GCE, (b) Br-Py/GCE, (c) AuNP-Si4Pic^{+}Cl^{-}/Br-Py/GCE, (d) ab-cTnT/AuNP-Si4Pic^{+}Cl^{-}/Br-Py/GCE, (e) gly/ab-cTnT/AuNP-Si4Pic^{+}Cl^{-}/Br-Py/GCE.

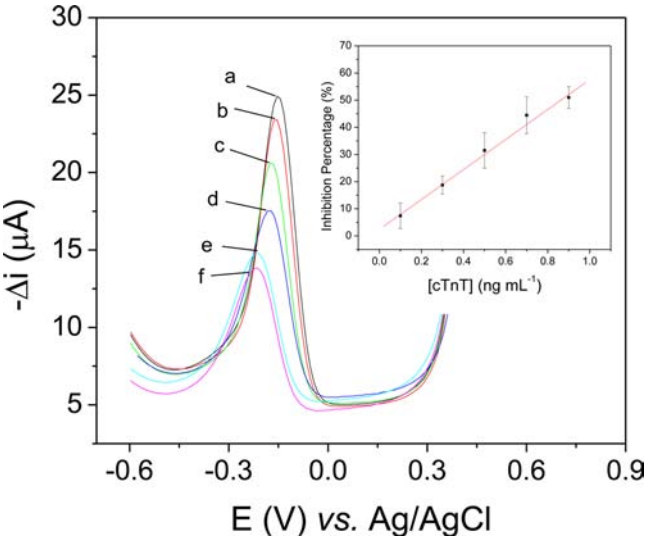

Figure 6. Square-wave voltammograms for (a) base peak, (b) 0.1 ng mL^{-1}, (c) 0.3 ng mL^{-1}, (d) 0.5 ng mL^{-1}, (e) 0.7 ng mL^{-1}, and (f) 0.9 ng mL^{-1} of cTnT. Inset: calibration curve.

(R) of 0.997, where I.P. is the inhibition percentage (%) and [cTnT] is the cardiac troponin concentration (ng mL^{-1}). The calculated limit of detection (LOD = three times the standard deviation of the intercept/slope) was found to be 0.076 ng mL^{-1}. According to the World Health Organization, healthy individuals have blood cTnT levels of ≤0.01 ng mL^{-1}. Furthermore, 0.3 ng mL^{-1} of cTnT has been established as the criterion for the diagnosis of myocardial infarction based on this biomarker. At around 3 to 4 h after the onset of myocardial injury the blood level of cTnT surpasses 0.3 ng mL^{-1}. Thus, the linear range for cTnT (0.1 ng mL^{-1} to 0.9 ng mL^{-1}) used in this study is sufficient to differentiate between healthy individuals and those with myocardial infarction.[26]

The reproducibility of the proposed immunosensor was evaluated by detecting 0.5 ng mL^{-1} of cTnT and the relative standard deviation (RSD) for six individual measurements was 8.0%, verifying the accuracy of the proposed method. The stability of the immunosensor was evaluated over a period of approximately 15 days with the electrode stored under refrigeration at 4 °C. The same level of response inhibition was obtained with the stored electrode and the signal variation was 2.9% after the 15-day evaluation period.

Table 2 summarizes the results obtained with cardiac troponin biosensors based on various methods and materials.

Table 2. Comparison of the Different Troponin Biosensors Based on Various Methods and Materials[a]

methods	material	linear range (ng mL^{-1})	LOD (ng mL^{-1})	incubation time (min)	reference
CV and EIS	CNF	0.1−100	0.2	60	27
ELC	Luminol-AuNP	0.1−1000	0.06	40	28
CV	o-PD/Au	0.009−0.8	0.009	10	29
SAW	AuNP	0.01−25	0.0067	20	30
ASV	Mesoporous material	0.8−5.0	0.5	30	31
FET	Si nanowire	0.096−46	0.092	-	32
SWV	LC/AuNP/GCE	0.1−0.9	0.076	10	This work

[a]CV: cyclic voltammetry; EIS: electrochemical impedance spectroscopy; CNF: carbon nanofiber; ELC: electrochemiluminescence; AuNP: gold nanoparticles; o-PD: *o*-phenylenediamine; Au: gold electrode; SAW: surface acoustic wave; ASV: anodic stripping voltammetry; FET: field-effect transistors; SWV: square-wave voltammetry; LC: liquid crystal; GCE: glassy carbon electrode.

It can be observed in this table that the proposed immunosensor has a relatively wide linear dynamic range and low detection limit for the determination of cTnT with respect to previously reported data. In addition, the analysis time associated with this immunosensor is short, which makes it an extremely attractive technique, especially for use as a point-of-care device.

Troponin Detection and Potential Interferents. The analytical response was obtained on incubating the immunosensor in synthetic serum spiked with cTnT (0.3 ng mL^{-1}) or human blood plasma containing 0.3 ng mL^{-1}. The results for the samples analyzed are given in Table 3.

To investigate possible interferents, a study was carried out with six potentially interfering compounds in the simulated serum. The results in Table 4 show a low degree of interference for most of the species tested in relation to the control test

dx.doi.org/10.1021/bc500341a | *Bioconjugate Chem.* 2014, 25, 1638−1643

Table 3. Cardiac Troponin Detection

sample	[cTnT] detected (ng mL^{-1})
Synthetic serum (0.3 ng mL^{-1})	0.26 ± 0.17
Synthetic serum (0.3 ng mL^{-1})	0.26 ± 0.01
Synthetic serum (0.3 ng mL^{-1})	0.32 ± 0.26
Blood plasma (0.3 ng mL^{-1})	0.28 ± 0.01

Table 4. Study of Potentially Interfering Compounds

compound[a]	percentage of interference (%)
creatine	12.6
creatinine	6.4
uric acid	8.2
glucose	8.2
ascorbic acid	1.9
BSA	1.3

[a]Tested individually; Average percentage interference in simulated serum: 7%.

(<10%). Only creatine caused a notable decrease in the signal peak (slightly greater than 10%).

CONCLUSIONS

In this study a nanostructured immunosensor obtained through the combination of Br-Py liquid crystalline molecule and AuNPs stabilized in a silsesquioxane matrix provided important advantages in the search for a highly sensitive analytical method for cTnT, an important biomarker for acute myocardial infarction detection. The results indicate that the immunosensor is able to detect a clinical level of cTnT and thus represents a useful tool for AMI diagnosis, indicating that this methodology could be used as a complementary approach in laboratory assays or point-of-care tests.

EXPERIMENTAL SECTION

Reagents and Solutions. The cTnT and ab-cTnT were purchased from Sigma–Aldrich. All reagents were of analytical grade and used without further purification and all solutions were prepared with deionized water obtained from a Milli-Q system (Millipore, Bedford, USA) at a resistivity of 18.2 MΩ cm^{-1}. The phosphate buffer saline (PBS) (0.01 mol L^{-1}, pH 7.4) used as the supporting electrolyte was prepared by dissolving KCl, NaCl, KH_2PO_4, and Na_2HPO_4 in double-distilled water and the pH value was adjusted with phosphoric acid or sodium hydroxide. The AuNP-Si4Pic$^+$Cl$^-$ nanoparticles were synthesized as described by Silva and co-workers:[16] 5 μL of 0.1 mol L^{-1} chloroauric acid was added to 2.5 mL of an aqueous solution of Si4Pic$^+$Cl$^-$ (2 g L^{-1}). The mixture was stirred for 5 min at room temperature and 200 μL of a freshly prepared 20 mmol L^{-1} sodium borohydride solution was quickly added under continuous stirring. After 60 s the solution changed from colorless to red, indicating the formation of AuNPs. AuNP-Si4Pic$^+$Cl$^-$ characterization carried out by transmission electronic microscopy (TEM) showed that the synthesized AuNPs were spherical in shape with an average diameter of 5.0 ± 0.2 nm, good distribution in the Si4Pic$^+$Cl$^-$ polymer, and the formation of some aggregates. The synthesis and complete characterization of the ionic liquid crystalline molecule Br-Py have been previously reported by Zapp and co-workers.[7] The synthetic serum was prepared using a PBS solution with the addition of ascorbic acid (5 mg L^{-1}), BSA (40 mg L^{-1}), citric acid (25 mg L^{-1}), creatinine (4.2 mg L^{-1}), creatine (10.7 mg L^{-1}), glycine (17.7 mg L^{-1}), glucose (830 mg L^{-1}), lysine (29.5 mg L^{-1}), and uric acid (40 mg L^{-1}). Human blood plasma purchased from Sigma–Aldrich containing 0.3 ng mL^{-1} of cTnT was used as a real sample.

Apparatus. Voltammetry (cyclic and square-wave) and electrochemical impedance spectroscopy (EIS) were performed using an Autolab PGSTAT128N potentiostat/galvanostat (Eco Chemie, The Netherlands) with an FRA impedance module and equipped with a three-electrode system. The working electrode was a glassy carbon electrode (GCE, surface area 2.0 mm^2) modified with ab-cTnT/AuNP-Si4Pic$^+$Cl$^-$/Br-Py (cTnT immunosensor). A platinum wire was used as the counter electrode and Ag/AgCl (3.0 mol L^{-1} KCl) as the reference electrode against which all potentials were measured and reported in these studies. Scanning electron microscopy (SEM) was performed using a JEOL JSM-6701 field emission gun (FEG) microscope (accelerating voltage of 10 kV). The AuNP-Si4Pic$^+$Cl$^-$ dispersion was deposited on a carbon-coated copper grid and analyzed using a JEOL JEM-2100 transmission electron microscope operating at 100 kV. Both types of microscopy were performed at the Central Laboratory for Electron Microscopy, Federal University of Santa Catarina (Florianópolis, Brazil). AuNP and ab-cTnT/AuNP zeta potential measurements were obtained using a Zetasizer Nano ZS instrument (Malvern Instruments, UK).

Immunosensor Preparation and Immunoassay Procedure. Before carrying out the Br-Py casting on the GCE, the electrode surface was polished with 0.05 μm alumina powder on a flat pad for 2 min and rinsed with deionized water. To remove the residual alumina particles the surface was ultrasonically cleaned in water for 10 min. Next, 3 μL (1×10^{-3} mol L^{-1} in CH_2Cl_2) of Br-Py solution was dropped onto the GCE and the solvent was allowed to evaporate in air. In the second step, a film of AuNP-Si4Pic$^+$Cl$^-$ was dripped onto the electrode surface and the solvent was evaporated. Next, the electrode was incubated with 3 μL (150 ng mL^{-1}) of ab-cTnT, and after 30 min the electrode surface was washed with PBS to remove nonimmobilized antibody molecules. The immunosensor was then incubated with 3 μL (0.01 mol L^{-1}) of glycine to block nonspecific sites on the surface of the sensor. An immunoassay was performed with simulated serum containing cTnT (0.1, 0.3, 0.5, 0.7, and 0.9 ng mL^{-1}) in sterile Eppendorfs to obtain the incubation solution. The cTnT immunosensor was then incubated for 10 min at room temperature (25 °C) with 3 μL of the sample solution. The Br-Py immunosensor was then thoroughly rinsed with PBS. Cyclic voltammograms for the immunosensor characterization were obtained in the potential range of +0.6 to −0.6 V and square-wave voltammograms for the cTnT determination were obtained from +0.4 to −0.6 V at a frequency of 100 Hz, amplitude of 80 mV, and step potential of 10 mV.

AUTHOR INFORMATION

Corresponding Author

*E-mail: zapp.edu@gmail.com.

Author Contributions

The manuscript was written with contributions from all authors. All authors have approved the final version of the manuscript.

Notes

The authors declare no competing financial interest.

■ ACKNOWLEDGMENTS

Financial support from FAPESC/CNPq (Process 2807/2012 − PRONEM), FAPESC/CNPq/PRONEX and also the scholarships granted by CNPq to E.Z., CAPES to P.S.S., and CAPES/PNPD to E.W. are gratefully acknowledged. This research was also supported by LCME−UFSC.

■ REFERENCES

(1) Demus, D., Goodby, J. W., Gray, G. W., Spiess, H.-W., Vill, V. (1979) *Handbook of Liquid Crystals*, Wiley-VCH, Weinheim.

(2) Han, Y., Chen, Z., Cao, D., Yu, J., Li, H., He, X., Zhang, J., Luo, Y., Lu, H., Tang, J., and Huang, H. (2014) Side-polished fiber as a sensor for the determination of nematic liquid crystal orientation. *Sens. Actuators, B 196*, 663−669.

(3) Lagerwall, P. F., and Scalia, G. (2012) A new era for liquid crystal research: Applications of liquid crystals in soft matter nano-, bio- and microtechnology. *Curr. Appl. Phys. 12*, 1387−1412.

(4) Bushby, R. J., and Kawata (2011) Liquid crystals that affected the world: Discotic liquid crystals K. *Liq. Cryst. 38*, 1415−1426.

(5) Woltman, S. J., Jay, G. D., and Crawford, G. P. (2007) Liquid-crystal materials find a new order in biomedical applications. *Nat. Mater. 6*, 929−938.

(6) Silva, T. R., Westphal, E., Gallardo, H., and Vieira, I. C. (2014) Ionic organic film sensor for determination of phenolic compounds. *Electroanalysis*, DOI: 10.1002/elan.201400197.

(7) Zapp, E., Westphal, E., Gallardo, H., Souza, B., and Vieira, I. C. (2014) Liquid crystal and gold nanoparticles applied to electrochemical immunosensor for cardiac biomarker. *Biosens. Bioelectron. 59*, 127−133.

(8) Liu, D., and Jang, C.-H. (2014) A new strategy for imaging urease activity using liquid crystal droplet patterns formed on solid surfaces. *Sens. Actuators, B 193*, 770−773.

(9) Campbell, F. W., and Compton, R. G. (2010) The use of nanoparticles in electroanalysis: an updated review. *Anal. Bioanal. Chem. 396*, 241−259.

(10) Pingarrón, J. M., Yáñez-Sedeño, P., and González-Cortés, A. (2008) Gold nanoparticle-based electrochemical biosensors. *Electrochim. Acta 53*, 5848−5866.

(11) Iost, R. M., and Crespilho, F. N. (2012) Layer-by-layer self-assembly and electrochemistry: applications in biosensing and bioelectronics. *Biosens. Bioelectron. 31*, 1−10.

(12) Yin, T., and Qin, W. (2013) Applications of nanomaterials in potentiometric sensors. *Trends Anal. Chem. 51*, 79−86.

(13) Menezes, E. W., Nunes, M. R., Arenas, L. T., Dias, S. L. P., Garcia, I. T. S., Gushikem, Y., Costa, T. M. H., and Benvenutti, E. V. (2012) Gold nanoparticle/charged silsesquioxane films immobilized onto Al/SiO_2 surface applied on the electrooxidation of nitrite. *J. Solid State Electrochem. 16*, 3703−3713.

(14) Nunes, M. R., Gushikem, Y., Landers, R., Dupont, J., Costa, T. M. H., and Benvenutti, E. V. (2012) Charged silsesquioxane used as a vehicle for gold nanoparticles to perform the synthesis of catalyst xerogels. *J. Sol-Gel Sci. Technol. 63*, 258−265.

(15) Fattori, N., Maroneze, C. M., Da Costa, L. P., Strauss, M., Mazali, I. O., and Gushikem, Y. (2013) Chemical and photochemical formation of gold nanoparticles supported on viologen-functionalized SBA-15. *Colloids Surf., A 437*, 120−126.

(16) Silva, P. S., Gasparini, B. C., Magosso, H. A., and Spinelli, A. (2014) Gold nanoparticles hosted in a water-soluble silsesquioxane polymer applied as a catalytic material onto an electrochemical sensor for detection of nitrophenol isomers. *J. Hazard. Mater. 273*, 70−77.

(17) Pedrero, M., Campuzano, S., and Pingarrón, J. M. (2014) Electrochemical Biosensors for the Determination of Cardiovascular Markers: a Review. *Electroanalysis 26*, 1132−1153.

(18) Qureshi, A., Gurbuz, Y., and Niazi, J. H. (2012) Biosensors for cardiac biomarkers detection: A review. *Sens. Actuators, B 171−172*, 62−76.

(19) Gomes-Filho, S. L. R., Dias, A. C. M. S., Silva, M. M. S., Silva, B. V. M, and Dutra, R. F. (2013) A carbon nanotube-based electrochemical immunosensor for cardiac troponin T. *Microchem. J. 109*, 10−15.

(20) Dutra, R. F., Mendes, R.K., Silva, V. L., and Kubota, L. T. (2007) Surface plasmon resonance immunosensor for human cardiac troponin T based on self-assembled monolayer. *J. Pharm. Biomed. Anal. 43*, 1744−1750.

(21) Wan, Y., Su, Y., Zhu, X., Liu, X., and Fan, C. (2013) Development of electrochemical immunosensors towards point of care diagnostics. *Biosens. Bioelectron. 47*, 1−11.

(22) Zhao, X., Pan, F., Garcia-Gancedo, L., Flewitt, A. J., Ashley, G. M., Luo, J., and Lu, J. R. (2012) Interfacial recognition of human prostate-specific antigen by immobilized monoclonal antibody: effects of solution conditions and surface chemistry. *J. R. Soc. Interface 9*, 2457−2467.

(23) Tarakanova, Y. N., Dmitriev, D. A., Massino, Y. S., Smirnova, M. B., Segal, O. L., Fartushnaya, O. V., Yakovleva, D. A., Kolyaskina, G. I., Lavrov, V. F., and Dmitriev, A. D. (2012) Effect of conditions of monoclonal antibody adsorption on antigen-binding activity. *Appl. Biochem. Microbiol. 48*, 506−512.

(24) Mattos, A. B., Freitas, T. A., Silva, V. L., and Dutra, R. F. (2012) A dual quartz crystal microbalance for human cardiac troponin T in real time detection. *Sens. Actuators, B 161*, 439−446.

(25) Yang, Y., Unnikrishnan, B., and Chen, S. (2011) Amperometric determination of 4-nitrophenol at multi-walled carbon nanotube-poly(diphenylamine) composite modified glassy carbon electrode. *Int. J. Electrochem. Sci. 6*, 3902−3912.

(26) Fonseca, R. A. S, Ramos-Jesus, J., Kubota, L. T., and Dutra, R. F. (2011) A Nanostructured piezoelectric immunosensor for detection of human cardiac troponin T. *Sensors 11*, 10785−10797.

(27) Periyakaruppan, A., Gandhiraman, R. P., Meyyappan, M., and Koehne, J. E. (2013) Label-free detection of cardiac troponin I using carbon nanofiber based nanoelectrode arrays. *Anal. Chem. 85*, 3858−3863.

(28) Li, F., Yu, Y., Cui, H., Yang, D., and Bian, Z. (2013) Label-free electrochemiluminescence immunosensor for cardiac troponin I using luminol functionalized gold nanoparticles as a sensing platform. *Analyst 138*, 1844−1850.

(29) Karimian, N., Vagin, M., Zavar, M. H. A., Chamsaz, M., Turner, A. P. F., and Tiwari, A. (2013) An ultrasensitive molecularly-imprinted human cardiac troponin sensor. *Biosens. Bioelectron. 50*, 492−498.

(30) Lee, W., Jung, J., Hahn, Y. K., Kim, S. K., Lee, Y., Lee, J., Lee, T., Park, J., Seo, H., Lee, J. N., Oh, J. H., Choi, Y., and Lee, S. S. (2013) A centrifugally actuated point-of-care testing system for the surface acoustic wave immunosensing of cardiac troponin I. *Analyst 138*, 2558−2566.

(31) Guo, H., He, N., Ge, S., Yang, D., and Zhang, J. (2005) MCM-41 mesoporous material modified carbon paste electrode for the determination of cardiac troponin I by anodic stripping voltammetry. *Talanta 68*, 61−66.

(32) Kong, T., Sul, R., Zhang, B., Zhang, Q., and Cheng, G. (2012) CMOS-compatible, label-free silicon-nanowire biosensors to detect cardiac troponin I for acute myocardial infarction diagnosis. *Biosens. Bioelectron. 34*, 267−272.